Biophysical Chemistry 184 (2013) 17–21

Contents lists available at ScienceDirect

Biophysical Chemistry

journal homepage: http://www.elsevier.com/locate/biophyschem

Replica exchange molecular dynamics simulations of an α/β-type small acid soluble protein (SASP)

P. Ojeda-May *, Jingzhi Pu *

Department of Chemistry and Chemical Biology, Indiana University–Purdue University Indianapolis, 402 N. Blackford Street, Indianapolis, IN 46202, USA

HIGHLIGHTS

- We investigated the thermodynamic properties of the intrinsic disordered α/β-type small acid soluble protein (SASP).
- We found a small free energy barrier of 1 kcal/mol separating the conformational ensembles at high and low temperatures.
- Residual structures and a high degree of plasticity were detected along the protein chain.

GRAPHICAL ABSTRACT

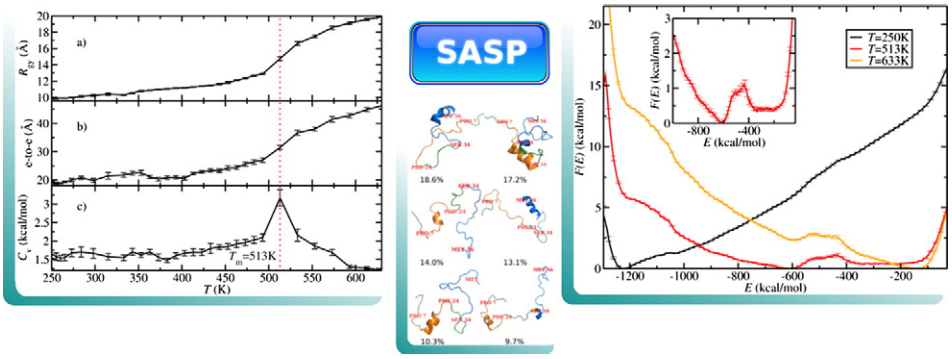

ARTICLE INFO

Article history:
Received 10 July 2013
Received in revised form 30 July 2013
Accepted 31 July 2013
Available online 20 August 2013

Keywords:
MD simulations
Proteins
Molecular simulation
Intrinsic disordered protein

ABSTRACT

Small acid soluble proteins (SASPs) of α/β-type play a major role in the resistance of spore DNAs to external assaults. It has been found that α/β-type SASP exhibits intrinsic disorder on isolation, but it acquires a defined native state upon binding to DNA. This disorder to order transition is not yet understood. Other questions related to the role of the thermodynamics and structure of the individual protein in the complex formation remain elusive. Characterization of the unbound state of α/β-type SASP in experiments could be a challenging problem because of the heterogeneous nature of the ensemble. Here, computer simulations can help gain more insights into the unbound state of α/β-type SASP. In the present work, by using replica exchange molecular dynamics (REMD), we simulated an α/β-type SASP on isolation with an implicit solvent. We found that α/β-type SASP undergoes a continuous phase transition with a small free energy barrier, a common feature of intrinsically disordered proteins (IDPs). Additionally, we detected the presence of residual α-helical structures at local level and a high degree of plasticity in the chain which can contribute to the fast disorder to order transition by reducing the fly-casting mechanism.

1. Introduction

Small acid soluble proteins (SASPs) of α/β-type are the major agents responsible for the resistance of spores of *Bacillus* and *Clostridium* to damaging factors such as heat, radiation and enzymes [1,2]. Binding of SASPs to spore DNA alters the conformational structure and photoreactivity of DNA [2,3], making it less sensitive to external assaults. The binding protein also undergoes major structural changes as revealed by circular dichroism spectroscopy studies [2]. These studies have shown that the isolated α/β-type SASP exhibits behaviors of an intrinsically disordered protein

* Corresponding authors. Tel.: +1 317 278 5721; fax: +1 317 274 4701.
E-mail addresses: pojedama@iupui.edu (P. Ojeda-May), jpu@iupui.edu (J. Pu).

0301-4622/$ – see front matter © 2013 Elsevier B.V. All rights reserved.
http://dx.doi.org/10.1016/j.bpc.2013.07.014

(IDP), devoid of a well-defined native state. However, when DNA is present, it folds to adopt a conformation with a large amount of α-helical secondary structure (~56–69%). The disorder to order transition of this binding protein is not yet understood [2].

DNA–α/β-type SASP complex was studied previously in detail regarding its thermodynamic and kinetic properties in equilibrium [2]. However, very little is known about the structure and dynamics of the isolated protein and its role in the complex formation. Further studies of α/β-type SASP could provide more insights into the global binding process based upon energetic/structural considerations.

The crystal structure of the bound state of α/β-type SASP was obtained very recently showing a helix–turn–helix (HTH) motif [2]. Obtaining information about the unbound conformational ensemble of α/β-type SASP can be a challenging problem in experiments because of the difficulty associated with monitoring the rapid changes of this heterogeneous ensemble. Here, modern computer simulations offer a suitable set of tools to explore structures and dynamics of the unbound conformations of SASP.

In this work, we studied the thermodynamic and conformational properties of the unbound state of the minor *Bacillus subtilis* α/β-type SASP [4], SspC$^{\Delta N11\text{-}D13K\text{-}C3}$, with Replica Exchange Molecular Dynamics (REMD) simulations using an implicit solvent model [5]. In what follows, we will refer to this protein simply as α/β-type SASP. The free energy landscape of the protein was analyzed through the weighted histogram method [6–8]. In addition to this, we characterized the high dimensional conformational space sampled for α/β-type SASP by using the clustering techniques.

2. Methods

2.1. Initial configuration

The initial configuration of the α/β-type SASP *B. subtilis* SspC$^{\Delta N11\text{-}D13K\text{-}C3}$ was obtained from the crystal structure of the SASP-DNA complex from Ref. [1] (PDB ID: 2Z3X). This α/β-type SASP variant is a 64 amino acid sequence engineered to bind more tightly to DNA than does the wild type SspC^{wt}. Seven residues from this sequence were not reported in the final PDB structure file and therefore they were not included in our simulation setup.

Chemistry at HARvard Macromolecular Mechanics (CHARMM) package [9] (version c36a1) was used to perform the simulations. Covalent bonds involving hydrogens were constrained with the SHAKE algorithm [10]. Electrostatic and van der Waals interactions were computed with the spherical atom-based cutoff method using a cutoff distance of 14 Å. Atom pairs that are separated by 1 or 2 covalent bonds are excluded from the non-bonded interactions. The atom pairs separated by 3 bonds (1–4 pairs) are included in the non-bonded list with a scale factor of 1.0. The CHARMM22 [11] force field was used to define molecular mechanical parameters in the simulations. Solvent effects were considered through the implicit solvent model Fast Analytical Continuum Treatment of Solvation (FACTS) [5]. The dielectric constant and the surface tension parameter were set to 1.0 and 0.015 kcal/(mol Å^2), respectively.

The initial structure of the protein was minimized with 30 steps using the adopted basis Newton–Raphson (ABNR) method [9] followed by 50 ps of equilibration simulations at each temperature before REMD simulations.

2.2. REMD simulations

REMD simulations were conducted with the ENSEMBLE module in CHARMM. The simulation was carried out with R=32 replicas (1 per processor) running on 2 GHz AMD Opteron processors. The customized scale of temperatures ranging from $T_{min} = 250$ K to $T_{max} = 633$ K, as shown in Table S1, was used to ensure a good sampling of the conformational space. As a remark, a similar range of temperatures was previously used in REMD simulations of proteins of similar size [12,13]. Exchanges between local copies i and $j = i + 1$ and non-local copies (see Table S2) were attempted every 1 ps according to the Metropolis criterion with probability,

$$w\left(C^{old}\rightarrow C^{new}\right) = \min\left\{1, exp\left[-\beta_i E\left(C_j\right) - \beta_j E(C_i) + \beta_i E(C_i) + \beta_j E\left(C_j\right)\right]\right\} \quad (1)$$

where $E(C_q)$ is the configurational energy of replica q and $\beta_q = (1/k_B T_q)$ is the inverse of temperature times the Boltzmann factor $k_B = 0.0019872$ kcal/mol K. Non-local moves were included in the simulation to allow the direct exchange between configurations at low and high temperatures.

Data production was performed for 24 ns REMD simulations, during which positions and energies were collected every 1,000 and 10 steps respectively. The final ensemble for each temperature contained 24,000 frames for subsequent data analysis.

2.3. Data analysis

Thermodynamics of α/β-type SASP was analyzed through the values of the radius of gyration (R_{gy}), the end-to-end distance (e-to-e) between C_α carbons, the constant volume specific heat (C_v) and the free energy profile [$F(E)$].

Specific heat C_v was computed according to the statistical mechanics equation [8],

$$C_v(T) = \frac{<E^2> - <E>^2}{k_B T^2} \quad (2)$$

where the symbol <> denotes average over the ensemble at temperature T and E is the configurational energy of a protein chain.

Free energy profiles where computed with the weighted histogram analysis method (WHAM) [6–8]. In this method, the range of configurational energies is discretized in bins of width Δ. In our case, the energy range was [−1300:0] kcal/mol and Δ = 6 kcal/mol, giving a total of 216 bins. A histogram of energies, $H(E)$, for each replica is updated each time an energy bin is visited during the simulation. Energy histograms are then used to compute the probability distribution at the temperature of interest T,

$$P_\beta(E) = \frac{\sum_{i=1}^{R} H_i(E) exp(-\beta E)}{\sum_{j=1}^{R} n_j exp\left(f_j - \beta_j E\right)} \quad (3)$$

where $H_i(E)$ is the energy histogram for replica i, and $\beta = 1/k_B T$ is the inverse of the desired temperature times the Boltzmann factor k_B. $\beta_j = 1/k_B T_j$ is the inverse of temperature for replica j and n_j is the total number of samples for the histogram of replica j. Because the free energy f_j (scaled by β_j) is not known a priori, it has to be computed self-consistently with a second equation,

$$exp\left(-f_j\right) = \sum_E P_\beta(E) \quad (4)$$

convergence is achieved when all entries of f_j change less than 10^{-5} with respect to previous iteration step. Finally, the free energy profile is computed as,

$$F(E) = -k_B T ln P_\beta(E). \quad (5)$$

Error bars were computed with the standard Jackknife method [14]. In this method, one block of data (1,000 frames in our case) is removed at a time from the data set (initially 24,000 frames). Then, all properties (e-to-e distance, R_{gy}, C_v and free energy profiles $F(E)$) are computed from the reduced data set. The operation of

ignoring consecutive blocks of data is repeated 24 times (=24000/1000). Averages of the properties (denoted by $\bar{f}$) are then obtained from these 24 subsets of data. Finally, errors are computed as,

$$\sigma = \sqrt{N-1}\sigma_f \tag{6}$$

where $N = 24$ and

$$\sigma_f^2 = \overline{(f)^2} - \left(\bar{f}\right)^2 \tag{7}$$

with f being the property of interest. The averages are given by

$$\overline{(f)^2} = \frac{1}{N}\sum_{i=1}^{N} f_i^2 \tag{8}$$

$$\bar{f} = \frac{1}{N}\sum_{i=1}^{N} f_i. \tag{9}$$

Reduction of the high-dimensional space of conformations of α/β-type SASP was accomplished with the aid of principal components analysis (PCA) [15,16], the defined secondary structure of proteins (DSSP) method [17] and the clustering algorithm Art-2 [18,19].

PCA was conducted using the root mean square deviation between any two structures (previous alignment) to compute the initial data matrix. After diagonalization, the eigenvalues were arranged in a descending order. Only the first four eigenvalues were used to project the data matrix in the new set of axes.

DSSP analysis, as implemented in the COOR SEC module of CHARMM, was used to compute the persistence of α-helix and β-sheet features along the protein chain. The fraction of secondary structure per residue was obtained as an average over the whole simulation time.

Characterization of the population of protein conformations at the melting temperature T_m was achieved by using the clustering algorithm implemented in the CLUSTER module of CHARMM. Time series of backbone dihedral angles ϕ and ψ were employed with a radius of 98° for pattern recognition.

3. Results and discussion

The plots of the radius of gyration and the end-to-end distance as a function of temperature show a step-wise behavior characteristic of a finite size phase transition [20] (see Fig. 1a–b). The curve of the specific heat, plotted in Fig. 1c, also shows a transition-like behavior signaled by a peak at the melting temperature $T_m = 513$ K (marked as a dotted line on the figure). The melting temperature T_m is well inside our selected range of temperatures ($T_{min} << T_m << T_{max}$), allowing for efficient capture of the crossing of conformational barriers from the folded ($T < T_m$) to the unfolded ($T > T_m$) ensembles. T_m is still much higher than the physiological melting temperatures of common proteins ~320 K [21–23]. This can be caused by either the protein force field or the implicit treatment of solvent [13,12].

The radius of gyration for the lowest temperature used (T_{min}) is ~ 9.8 Å, and it increased roughly by a factor of 2 (~ 19.9 Å) for the highest temperature (T_{max}). As for the end-to-end distance, we found that the average value for high temperatures (~46.4 Å) is approximately 2.4 times higher than the value at low temperatures (~19.1 Å), indicating that, on average, the structures are relatively compact at low temperatures. Interestingly, the average radius of gyration for high temperatures is much smaller than the maximum value observed during the whole simulation (~140 Å). Thus, both the radius of gyration and the end-to-end distance parameters display a slow increasing behavior which resembles a continuous transition from an ensemble of unfolded to an ensemble of folded structures. This can also be observed from the low peak and broad curve of the specific heat in Fig. 1c. As a remark, continuous transitions are characterized by low (or zero) free energy barriers [24].

Regarding the energetics, the free energy profile of α/β-type SASP was computed at three different temperatures $T = 250$ K, 513 K and 633 K as shown in Fig. 2. At low temperatures ($T = 250$ K), only one ensemble of conformations is populated, which is reflected in the one-basin feature of $F(E)$. At the melting temperature T_m (513 K), we observed the presence of two minima associated with the unfolded and folded ensembles, which reveal the two-state nature of the process. However, because the energy barrier separating the two minima is small (~1.0 kcal/mol), the overall transition proceeds continuously (down-hill) rather than abruptly (two-state). Interestingly, small free energy barriers have been found previously in simulations of other IDPs [25]. In fact, small barriers seem necessary in IDPs because they allow the fast structure interconversion [26–31]without a high energetic cost. This fast interconversion mechanism can accelerate the folding of α/β-type SASP upon DNA binding, explaining the fast and efficient disorder to order transition observed in experiments. Finally, at high temperatures (e.g. 633 K) the profile exhibits a funnel-like shape with a single basin found for the unfolded ensemble.

The similarity of conformational ensembles at different temperatures was analyzed by means of the PCA method. The four eigenvalues with the highest variance accounted for the 99.0%, 2.0%, 1.9% and 1.6%

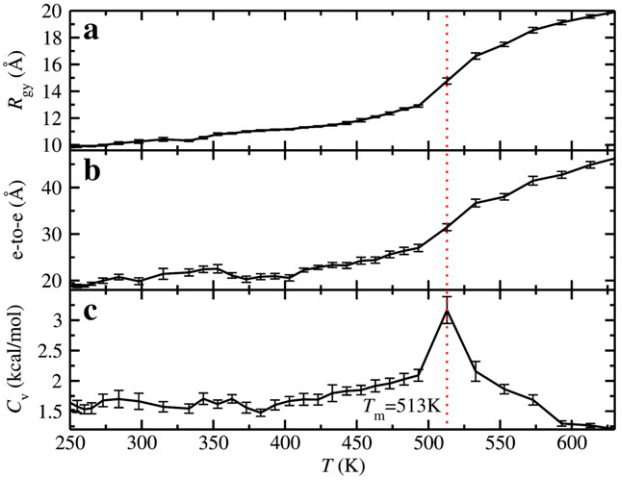

Fig. 1. Thermodynamic properties showing the finite size phase transition of α/β-type SASP: (a) radius of gyration (R_{gy}), (b) end-to-end distance (e-to-e) and (c) specific heat (C_v) as a function of temperature. The melting temperature T_m is denoted by a dotted line.

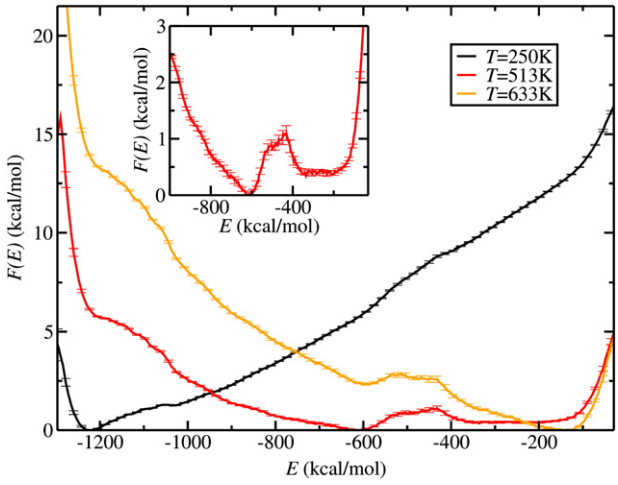

Fig. 2. Free energy profiles at temperatures $T = 250$ K, 513 K and 633 K. The inset plot shows the barrier height of ~1 kcal/mol at the melting temperature T_m.

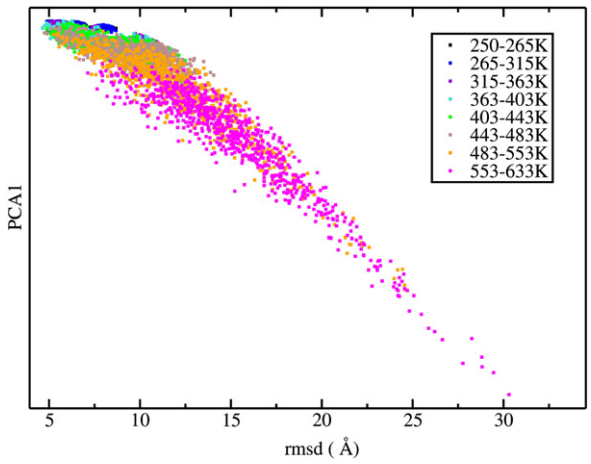

Fig. 3. First principal component as a function of the RMSD. Ensembles at different temperatures are located in the same region of the conformational space. Thus, small jumps can drive a conformation across ensembles.

of the total population, respectively. The first principal axis is plotted against the root mean square deviation (RMSD) in Fig. 3. We considered information from other axes redundant. We observed that all the ensembles are located in the same region of PCA-RMSD phase space with a shift along the first principal axis from low temperatures (top) to high temperatures (bottom). This indicates that no drastic structural rearrangements are needed for the protein conformers to visit various ensembles at different temperatures [32] and confirms the result of the continuous transition and the small free energy barrier obtained from the energetic considerations.

In what follows, we will focus on the ensemble at the melting temperature (T_m) because at this temperature, the folded and unfolded phases coexist. Special attention was paid to two helical regions of SASP, which play a major role in the tight-binding to DNA: the first helix (helix1) is located between residues Pro-7 and Phe-24 while the second helix (helix2) between residues Ser-34 and Met-56 [1].

The fraction of α-helical and β-sheet content per residue can be seen in Fig. 4. The high fraction of α-helical content at some residues indicates the presence of residual structures. In particular, residues Gln-15 and Lys-46 have a high propensity of 50% and 43.2%, respectively,

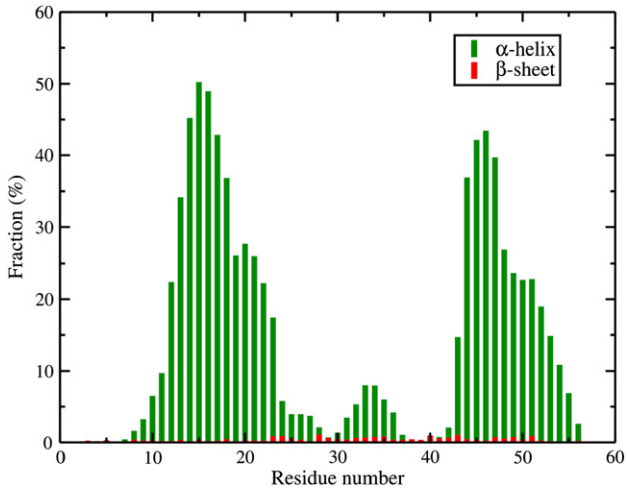

Fig. 4. Secondary structures found in α/β-type SASP. We observed the presence of a high local persistence of α-helical structures around residues 15 (Gln) and 46 (Lys).

to form α-helices. Our findings here suggest that these residues can act as hot spots in SASP to maintain certain α-helical features in the unbound state and may be essential for the protein to acquire the HTH structural motif in the DNA-bound form. This can explain why a mutation at the level of these residues can change topology of the protein [1]. It should be noticed that the hot spots in the present context have an entropic (conformational) origin rather than an enthalpic origin as in the hot spots studied in Ref. [33].

Residues close to Gln-15 and Lys-46 also have a high propensity for helical structures. A lower (but still detectable in simulations) peak related to α-helices was detected around Thr-33 (7.8%). It should be emphasized that even when there is a relatively high persistence of α-helical structures at local levels the helical content averaged over the entire chain is only ~14.3%. This fraction is presumably small for detection in experiments that measure an average signal over the chain rather than at specific residues. As a remark, these α-helical residual structures can help reduce the folding time and decrease the fly-fasting mechanism [28] upon DNA binding. Additionally, preformed structures can reduce the entropic penalty upon binding allowing for a simple conformational shift towards a bound-state ensemble [34]. Regarding the β-structures, the average fraction was negligible (<<1.0%) for all residues.

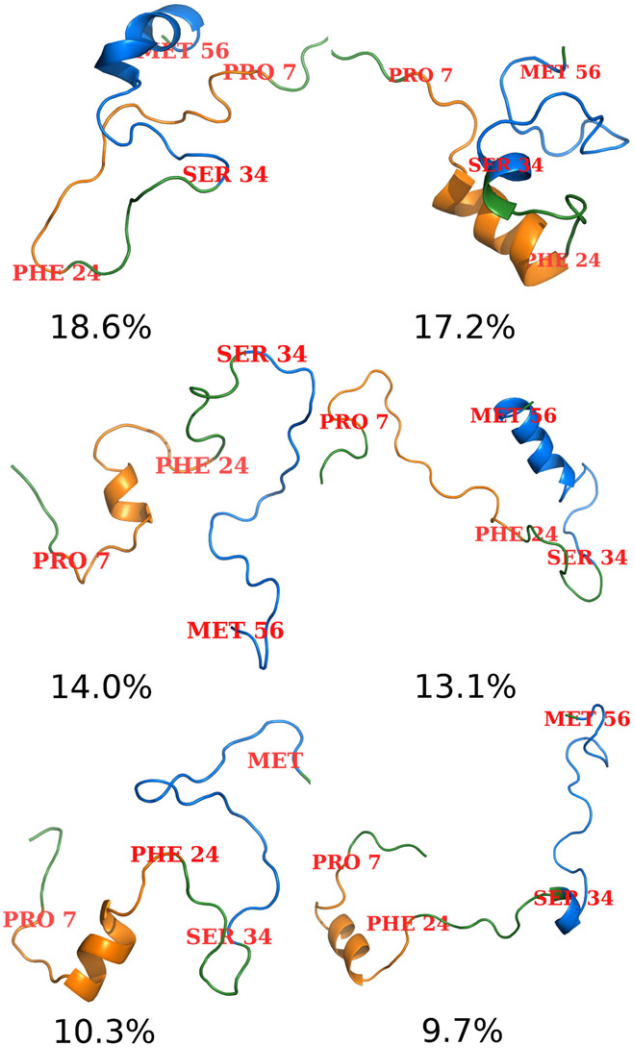

Fig. 5. Representative members in the clusters found at the simulated melting temperature T_m, with the statistical weights of the clusters shown. None of the cluster was predominant. Representative members display helical motifs. Ends of helix1 and helix2 are labeled on figure.

Representative members of the clusters obtained by performing a clustering analysis of α/β-type SASP are shown in Fig. 5. The reader can observe the presence of residual helical structures along helix1 and helix2 segments defined above.

The statistical weight was very similar for all clusters, indicating that none of them predominated in the ensemble at the melting temperature. Thus, the ensemble displays a high degree of plasticity as opposite to rigid ensembles of common proteins where one or two structures account for the ~80% of the total population [35]. Another indicator of the high plasticity of the ensemble was the high value for the selection pattern radius (98°) used to obtain less than ten well-populated clusters. For lower values none of the clusters consisted of more than 10 members.

4. Conclusions

By doing REMD simulations of the α/β-type SASP on isolation, we were able to gain more insight into the thermodynamics of the unbound ensemble. We found a finite size phase transition with a continuous character as revealed by common thermodynamics parameters. The free energy barrier height was small (1 kcal/mol), a common feature of IDPs. In addition to this, we found a high degree of plasticity in the chain at the melting temperature.

We were also able to gain more insight into the binding process to DNA: we found residual structures of helical type which can decrease the fly-casting mechanism upon binding.

Acknowledgements

We thank Prof. Lei Li for discussion. This work was supported by a start-up grant from Indiana University–Purdue University Indianapolis (IUPUI). The computing time was provided by High-Performance Computing Cluster funded by the School of Science at IUPUI and Indiana University BigRed High Performance Computing facilities, funded by the National Science Foundation (NSF).

Appendix A. Supplementary data

Supplementary data to this article can be found online at http://dx.doi.org/10.1016/j.bpc.2013.07.014.

References

[1] K.S. Lee, D. Bumbaca, J. Kosman, P. Setlow, M.J. Jedrzejas, Structure of a protein DNA complex essential for DNA protection in spores of bacillus species, Proc. Natl. Acad. Sci. 105 (8) (2008) 2806–2811, http://dx.doi.org/10.1073/pnas.0708244105.
[2] C.S. Hayes, Z.-Y. Peng, P. Setlow, Equilibrium and kinetic binding interactions between DNA and a group of novel, nonspecific DNA-binding proteins from spores of bacillus and clostridium species, J. Biol. Chem. 275 (45) (2000) 35040–35050, http://dx.doi.org/10.1074/jbc.M005669200.
[3] S.C. Mohr, N.V. Sokolov, C.M. He, P. Setlow, Binding of small acid-soluble spore proteins from *Bacillus subtilis* changes the conformation of DNA from b to a, Proc. Natl. Acad. Sci. 88 (1) (1991) 77–81(PMID: 1898779).
[4] P. Setlow, Spore germination, Curr. Opin. Microbiol. 6 (6) (2003) 550–556, http://dx.doi.org/10.1016/j.mib.2003.10.001.
[5] U. Haberthuer, A. Caflisch, FACTS: Fast analytical continuum treatment of solvation, J. Comput. Chem. 29 (5) (2008) 701–715, http://dx.doi.org/10.1002/jcc.20832.
[6] A.M. Ferrenberg, R.H. Swendsen, Optimized Monte Carlo data analysis, Phys. Rev. Lett. 63 (1989) 1195–1198, http://dx.doi.org/10.1103/PhysRevLett.63.1195.
[7] S. Kumar, J.M. Rosenberg, D. Bouzida, R.H. Swendsen, P.A. Kollman, The weighted histogram analysis method for free-energy calculations on biomolecules. I. The method, J. Comput. Chem. 13 (8) (1992) 1011–1021, http://dx.doi.org/10.1002/jcc.540130812.
[8] I.-C. Yeh, M.S. Lee, M.A. Olson, Calculation of protein heat capacity from replica-exchange molecular dynamics simulations with different implicit solvent models, J. Phys. Chem. B 112 (47) (2008) 15064–15073, http://dx.doi.org/10.1021/jp802469g.
[9] B.R. Brooks, C.L. Brooks, A.D. Mackerell, L. Nilsson, R.J. Petrella, B. Roux, Y. Won, G. Archontis, C. Bartels, S. Boresch, A. Caflisch, L. Caves, Q. Cui, A.R. Dinner, M. Feig, S. Fischer, J. Gao, M. Hodoscek, W. Im, K. Kuczera, T. Lazaridis, J. Ma, V. Ovchinnikov, E. Paci, R.W. Pastor, C.B. Post, J.Z. Pu, M. Schaefer, B. Tidor, R.M. Venable, H.L. Woodcock, X. Wu, W. Yang, D.M. York, M. Karplus, Charmm: the biomolecular simulation program, J. Comput. Chem. 30 (10) (2009) 1545–1614, http://dx.doi.org/10.1002/jcc.21287.
[10] J.-P. Ryckaert, G. Ciccotti, H.J. Berendsen, Numerical integration of the Cartesian equations of motion of a system with constraints: molecular dynamics of n-alkanes, J. Comput. Phys. 23 (3) (1977) 327–341, http://dx.doi.org/10.1016/0021-9991(77)90098-5.
[11] A.D. MacKerell, D. Bashford, M. Bellott, R.L. Dunbrack, J.D. Evanseck, M.J. Field, S. Fischer, J. Gao, H. Guo, S. Ha, D. Joseph-McCarthy, L. Kuchnir, K. Kuczera, F.T.K. Lau, C. Mattos, S. Michnick, T. Ngo, D.T. Nguyen, B. Prodhom, W.E. Reiher, B. Roux, M. Schlenkrich, J.C. Smith, R. Stote, J. Straub, M. Watanabe, J. Wiorkiewicz-Kuczera, D. Yin, M. Karplus, All-atom empirical potential for molecular modeling and dynamics studies of proteins, J. Phys. Chem. B 102 (18) (1998) 3586–3616, http://dx.doi.org/10.1021/jp973084f.
[12] S. Hoefinger, B. Almeida, U.H.E. Hansmann, Parallel tempering molecular dynamics folding simulation of a signal peptide in explicit water, Proteins Struct. Funct. Bioinforma. 68 (3) (2007) 662–669, http://dx.doi.org/10.1002/prot.21268.
[13] J. Zhang, W. Li, J. Wang, M. Qin, W. Wang, All-atom replica exchange molecular simulation of protein BBL, Proteins Struct. Funct. Bioinforma. 72 (3) (2008), http://dx.doi.org/10.1002/prot.22001.
[14] M.H. Quenouille, Approximate tests of correlation in time-series, J. R. Stat. Soc. Ser. B Methodol. 11 (1) (1949) 68–84.
[15] K. Pearson, Liii. on lines and planes of closest fit to systems of points in space, Philos. Mag. Ser. 6 2 (11) (1901) 559–572, http://dx.doi.org/10.1080/14786440109462720.
[16] H. Shirai, N. Nakajima, J. Higo, A. Kidera, H. Nakamura, Conformational sampling of CDR-H3 in antibodies by multicanonical molecular dynamics simulation, J. Mol. Biol. 278 (2) (1998) 481–496, http://dx.doi.org/10.1006/jmbi.1998.1698.
[17] W. Kabsch, C. Sander, Dictionary of protein secondary structure: pattern recognition of hydrogen-bonded and geometrical features, Biopolymers 22 (12) (1983) 2577–2637, http://dx.doi.org/10.1002/bip.360221211.
[18] G.A. Carpenter, S. Grossberg, Art 2: self-organization of stable category recognition codes for analog input patterns, Appl. Opt. 26 (23) (1987) 4919–4930, http://dx.doi.org/10.1364/AO.26.004919.
[19] M.E. Karpen, D.J. Tobias, C.L. Brooks, Statistical clustering techniques for the analysis of long molecular dynamics trajectories: analysis of 2.2-ns trajectories of ypgdv, Biochemistry 32 (2) (1993) 412–420, http://dx.doi.org/10.1021/bi00053a005.
[20] C.-Y. Lin, C.-K. Hu, U.H.E. Hansmann, Parallel tempering simulations of hp-36, Proteins Struct. Funct. Bioinforma. 52 (3) (2003) 436–445, http://dx.doi.org/10.1002/prot.10351.
[21] V. Muñoz, J.M. Sanchez-Ruiz, Exploring protein-folding ensembles: a variable-barrier model for the analysis of equilibrium unfolding experiments, Proc. Natl. Acad. Sci. U.S.A. 101 (51) (2004) 17646–17651, http://dx.doi.org/10.1073/pnas.0405829101.
[22] C.M. Johnson, Differential scanning calorimetry as a tool for protein folding and stability, Arch. Biochem. Biophys. 531 (12) (2013) 100–109, http://dx.doi.org/10.1016/j.abb.2012.09.008.
[23] A.N. Naganathan, R. Perez-Jimenez, V. Muñoz, J.M. Sanchez-Ruiz, Estimation of protein folding free energy barriers from calorimetric data by multi-model Bayesian analysis, Phys. Chem. Chem. Phys. 13 (38) (2011) 17064–17076, http://dx.doi.org/10.1039/C1CP20156E.
[24] F. Takagi, N. Koga, S. Takada, How protein thermodynamics and folding mechanisms are altered by the chaperonin cage: molecular simulations, Proc. Natl. Acad. Sci. 100 (20) (2003) 11367–11372, http://dx.doi.org/10.1073/pnas.1831920100.
[25] J. Mittal, T.H. Yoo, G. Georgiou, T.M. Truskett, Structural ensemble of an intrinsically disordered polypeptide, J. Phys. Chem. B 117 (1) (2013) 118–124, http://dx.doi.org/10.1021/jp308984e.
[26] K. Lindorff-Larsen, S. Piana, R.O. Dror, D.E. Shaw, How fast-folding proteins fold, Science 334 (6055) (2011) 517–520, http://dx.doi.org/10.1126/science.1208351.
[27] D.D. Boehr, R. Nussinov, P.E. Wright, The role of dynamic conformational ensembles in biomolecular recognition, Nat. Chem. Biol. 5 (11) (2009) 789–796, http://dx.doi.org/10.1038/nchembio.232.
[28] W. Zhang, D. Ganguly, J. Chen, Residual structures, conformational fluctuations, and electrostatic interactions in the synergistic folding of two intrinsically disordered proteins, PLoS Comput. Biol. 8 (1) (2012), http://dx.doi.org/10.1371/journal.pcbi.1002353.
[29] M.B. Prigozhin, M. Gruebele, Microsecond folding experiments and simulations: a match is made, Phys. Chem. Chem. Phys. 15 (10) (2013) 3372–3388, http://dx.doi.org/10.1039/C3CP43992E.
[30] J. Chen, Towards the physical basis of how intrinsic disorder mediates protein function, Arch. Biochem. Biophys. 524 (2) (2012) 123–131, http://dx.doi.org/10.1016/j.abb.2012.04.024.
[31] D. Ganguly, W. Zhang, J. Chen, Synergistic folding of two intrinsically disordered proteins: searching for conformational selection, Mol. Biosyst. 8 (2012) 198–209, http://dx.doi.org/10.1039/C1MB05156C.
[32] J. Higo, N. Ito, M. Kuroda, S. Ono, N. Nakajima, H. Nakamura, Energy landscape of a peptide consisting of α -helix, β -turn, and β -hairpin, and other disordered conformations, Protein Sci. 10 (6) (2001) 1160–1171, http://dx.doi.org/10.1110/ps.44901.
[33] X. Li, O. Keskin, B. Ma, R. Nussinov, J. Liang, Protein–protein interactions: hot spots and structurally conserved residues often locate in complemented pockets that pre-organized in the unbound states: implications for docking, J. Mol. Biol. 344 (3) (2004) 781–795, http://dx.doi.org/10.1016/j.jmb.2004.09.051.
[34] R. Pancsa, M. Fuxreiter, Interactions via intrinsically disordered regions: what kind of motifs? IUBMB Life 64 (6) (2012) 513–520, http://dx.doi.org/10.1002/iub.1034.
[35] W.-T. Chu, J.-L. Zhang, Q.-C. Zheng, L. Chen, H.-X. Zhang, Insights into the folding and unfolding processes of wild-type and mutated SH3 domain by molecular dynamics and replica exchange molecular dynamics simulations, PLoS ONE 8 (5) (2013) e64886, http://dx.doi.org/10.1371/journal.pone.0064886.